GEOLOGY | THE GEOLOGICAL SOCIETY OF AMERICA®

https://doi.org/10.1130/G46666.1

Manuscript received 16 June 2019
Revised manuscript received 15 September 2019
Manuscript accepted 2 October 2019

Published online 28 October 2019

Focused fluid seepage related to variations in accretionary wedge structure, Hikurangi margin, New Zealand

Sally J. Watson[1]*, Joshu J. Mountjoy[1], Philip M. Barnes[1], Gareth J. Crutchley[2,3], Geoffroy Lamarche[1,4], Ben Higgs[1,5], Jess Hillman[2], Alan R. Orpin[1], Aaron Micallef[6], Helen Neil[1], John Mitchell[1], Arne Pallentin[1], Tim Kane[1], Susi Woelz[1], David Bowden[1], Ashley A. Rowden[1,7] and Ingo A. Pecher[4]

[1]National Institute of Water and Atmospheric Research (NIWA), P.O. Box 14901, Kilbirnie, Wellington 6021, New Zealand
[2]GNS Science, P.O. Box 30368, Lower Hutt, Wellington 5040, New Zealand
[3]GEOMAR Helmholtz Centre for Ocean Research Kiel 24148, Germany
[4]School of Environment, University of Auckland, Auckland 1142, New Zealand
[5]Golder Associates, 214 Durham Street South, Christchurch 8011, New Zealand
[6]Marine Geology and Seafloor Surveying, Department of Geosciences, University of Malta, Msida MSD 1805, Malta
[7]School of Biological Sciences, Victoria University of Wellington, Wellington 6140, New Zealand

ABSTRACT

Hydrogeological processes influence the morphology, mechanical behavior, and evolution of subduction margins. Fluid supply, release, migration, and drainage control fluid pressure and collectively govern the stress state, which varies between accretionary and nonaccretionary systems. We compiled over a decade of published and unpublished acoustic data sets and seafloor observations to analyze the distribution of focused fluid expulsion along the Hikurangi margin, New Zealand. The spatial coverage and quality of our data are exceptional for subduction margins globally. We found that focused fluid seepage is widespread and varies south to north with changes in subduction setting, including: wedge morphology, convergence rate, seafloor roughness, and sediment thickness on the incoming Pacific plate. Overall, focused seepage manifests most commonly above the deforming backstop, is common on thrust ridges, and is largely absent from the frontal wedge despite ubiquitous hydrate occurrences. Focused seepage distribution may reflect spatial differences in shallow permeability architecture, while diffusive fluid flow and seepage at scales below detection limits are also likely. From the spatial coincidence of fluids with major thrust faults that disrupt gas hydrate stability, we surmise that focused seepage distribution may also reflect deeper drainage of the forearc, with implications for pore-pressure regime, fault mechanics, and critical wedge stability and morphology. Because a range of subduction styles is represented by 800 km of along-strike variability, our results may have implications for understanding subduction fluid flow and seepage globally.

INTRODUCTION

Fluids—in their gaseous or liquid phase—play a critical role in controlling the dynamics of accretionary wedges by influencing pore pressure (Dahlen, 1990; Saffer and Bekins, 2006) and the mechanical behavior of faults (Sibson, 1992; Kodaira et al., 2004; Liu and Rice, 2007; Bangs et al., 2015). Fluids are released from both the subducting plate and the accretionary wedge, due to compaction and thermally controlled mineral-phase transformations. Efficient fluid migration relies on the occurrence of high permeability, i.e., flow pathways through faults, fractures, and high-porosity lithologies (Saffer and Tobin, 2011; Plaza-Faverola et al., 2012; Bangs et al., 2015).

Despite their important role at subduction zones, subsurface fluids are difficult to quantify directly, although the seafloor manifestation of fluid flow is often observed as seeps (e.g., Judd and Hovland, 2009). Few studies have investigated seep distributions at a margin scale (e.g., Ranero et al., 2008; Sahling et al., 2008; Barnes et al., 2010; Geersen et al., 2018; Riedel et al., 2018).

The Hikurangi margin, offshore the North Island of New Zealand, exhibits evidence for widespread fluid seepage (Lewis and Marshall, 1996; Barnes et al., 2010; Greinert et al., 2010), together with variations in tectonic structure and processes capturing a range of subduction styles (Fig. 1). These variations include changes in the rate and obliquity of plate convergence (Wallace et al., 2004), occurrence of subducting seamounts, accretionary versus erosional subduction behavior, and wedge morphology (Lewis and Pettinga, 1993; Barnes et al., 2010). From south to north, the deformation setting changes from subduction to transform transition, to classical frontal accretion, and finally to widespread frontal tectonic erosion with seamount subduction. These changes accompany a northward reduction in sediment thickness on the subducting Pacific plate, from ~9 km (Fig. 1; Plaza-Faverola et al., 2012) to ~1–2 km (Barker et al., 2009, 2018). The margin attains a width of 150 km, characterized by a deforming Late Cretaceous–Paleogene presubduction foundation inboard of a late Cenozoic accretionary wedge (Lewis and Pettinga, 1993; Barnes et al., 2010; Ghisetti et al., 2016). Estimates of the average volume of fluids subducted and accreted along strike are high (~57 $m^3\ yr^{-1}\ m^{-1}$; Pecher et al., 2010), with a significant reduction expected northward, and the vast majority drained from the wedge (Ellis et al., 2015).

We investigated the distribution of focused fluid seepage using an exceptional high-quality regional data set from the Hikurangi margin, including: (1) hydro-acoustic data that image active gas bubbles; (2) seafloor camera observations of chemosynthetic seep ecosystems; and (3) geomorphological and seafloor acoustic

*E-mail: Sally.Watson@niwa.co.nz

CITATION: Watson, S.J., et al., 2020, Focused fluid seepage related to variations in accretionary wedge structure, Hikurangi margin, New Zealand: Geology, v. 48, p. 56–61, https://doi.org/10.1130/G46666.1

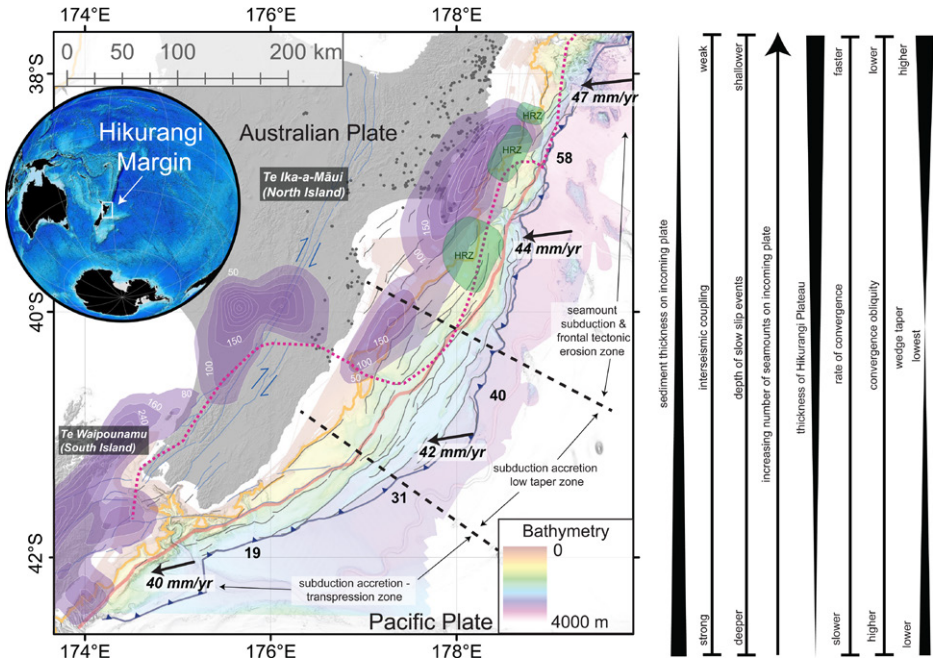

Figure 1. Hikurangi margin, offshore the North Island of New Zealand. Black dots are locations of onshore seepage (Campbell, 2006; Campbell et al., 2008). Colored region offshore represents the surveyed region (see the Data Repository [see footnote 1] for more detailed information on the extent of the multibeam echosounder [MBES] and water-column backscatter data coverage). North-to-south changes in tectonic structure and subduction processes that may be contributing to the distribution of fluid seepage on the seafloor are annotated on the map and detailed on schematic bars at right. Purple semitransparent contours represent total slip detected in slow slip events on the subduction interface since 2002 CE (contour values in mm). Pink dashed line is the boundary between strong interseismic coupling in the north and weak interseismic coupling in the south, determined by the coupling coefficient on the subduction interface (Wallace and Beavan, 2010; Wallace et al., 2018). Sem-itransparent green areas are high-amplitude reflectivity zones (HRZ) beneath the interface as interpreted in seismic reflection profiles (Bell et al., 2010). Bold black arrows are convergence vectors, with convergence rate below (Beavan et al., 2002); bold values adjacent to the deformation front are orthogonal convergence rates from Wallace et al. (2004, 2012). For Figures 1 and 2, major strike-slip faults (thin blue lines) and thrust faults (thin black lines) are displayed both onshore and offshore. Thick yellow line is 650 m depth contour representing the upper limit of gas hydrate stability in this region. Black dashed lines represent the boundaries between different tectonic domains on the margin (Lewis and Pettinga, 1993; Collot et al., 1996; Barker et al., 2009; Barnes et al., 2010; Fagereng, 2011). Pale red line is the backstop boundary denoting the boundary between deforming Late Cretaceous–Paleogene presubduction sequence and the frontal wedge, composed of late Cenozoic trench-fill sequences (Lewis and Pettinga, 1993; Barnes et al., 2010). Navy blue line represents the deformation front, with subduction teeth on the overriding plate (Barnes et al., 2010, 2018).

backscatter data indicative of substrates associated with focused fluid seepage (Fig. 2; see the GSA Data Repository[1] for individual presentation of seepage features, grid sizes, and observation thresholds). We used observed spatial patterns of seep distribution to map shallow-wedge permeability, and then we considered the implications for hydrological framework and subduction processes.

SEEP INDICATORS AND THEIR DISTRIBUTION ON THE HIKURANGI MARGIN

There is extensive evidence for both active and relict (or dormant) focused fluid seepage in water depths of 50–2400 m along the margin (Figs. 2A–2C). Pockmarks are widespread on the outer shelf and upper slope (28% of the database); however, very few pockmarks have concomitant indicators of seep activity and are not considered herein.

Active focused seepage was identified from hydro-acoustic flares and/or direct observations of live seep fauna (Figs. 2A–2C), commonly with characteristic rough seafloor geomorphology, high seafloor backscatter intensity, and mounds. Approximately 75% of authigenic carbonate observations were corroborated by evidence for active seepage (Fig. 2; see also the Data Repository).

Focused seepage occurs across the inboard margin, at sites located on the outer continental shelf, slope, and thrust ridges. Generally, seepage indicators are rare across the outer margin (Figs. 2A–2C and 3A–3C).

The northern margin is characterized by active, spatially concentrated fluid expulsion on the outer shelf and upper slope (including active pockmarks with coincident flares; seep site spatial density: ~1/17 km^2; Figs. 2A and 3A). For example, the Tuaheni Seep Field covers ~90 km^2 and includes >1700 seep indicators (including flares, mounds, and pockmarks) in water depths of 58–532 m, making it the most spatially concentrated and shallowest seep area observed anywhere on the margin (Fig. 2A; Higgs et al., 2019). Farther offshore, active seepage is scattered mainly along midslope ridges (Figs. 2A and 3A).

Approximately 5% (n = 161) of the seep occurrences were observed within the wide, central margin between Ōmakere and Urutī Ridges (Fig. 2B). Here, sparsely focused seeps are particularly rare at seafloor depths >650 m (Figs. 2A–2C; seep site spatial density: ~1/139 km^2), with only 19 hydro-acoustic flares and one seafloor observation of authigenic carbonate (Figs. 2B and 3B). Indications of active focused seepage are largely absent from the 70-km-wide frontal accretionary wedge.

Across the southern margin, active, sustained, and focused seepage is widespread but concentrated mainly on thrust ridges (Figs. 2C and 3C). The Glendhu and Honeycomb Ridges (~2100–2400 m water depths) are the only sites with evidence of active seepage at seafloor depths >2100 m and proximal to the deformation front (Fig. 2C). At the southern extent of the margin, seepage is widespread along the crest of Kekerengū Bank, while the southernmost seep site lies in the Kōwhai Sea Valleys (Fig. 2C).

RELATIONSHIP BETWEEN FLUID SEEPAGE AND MARGIN CHARACTERISTICS

The comprehensive spatial coverage and quality of our data are exceptional for subduction margins globally (e.g., Ranero et al., 2008; Geersen et al., 2018; Riedel et al., 2018). Hydro-acoustic flares are the most common seepage indicator (~46% of the database), indicative of active focused gas expulsion (Fig. 2).

The distribution of active focused seepage on the Hikurangi margin may reflect variations in the shallow permeability architecture of the wedge. Shallow fluid pathways may in turn reflect higher permeability at depth, governed by the regional tectonic framework (Figs. 2A–2C and 4A–4C). In the north, where the convergence rate is ~5 cm/yr, the Tuaheni Seep Field is spatially correlated with localized and possibly shallow extensional faulting (Böttner et al., 2018), immediately east of major thrust faults

[1]GSA Data Repository item 2020017, methodologies, equipment specifications, individual presentation of seepage features, grid sizes, and observation thresholds, and an MSExcel spreadsheet containing all fluid expulsion features presented in this study, with coordinates, depth and voyage/dataset reference, is available online at http://www.geosociety.org/datarepository/2020/, or on request from editing@geosociety.org.

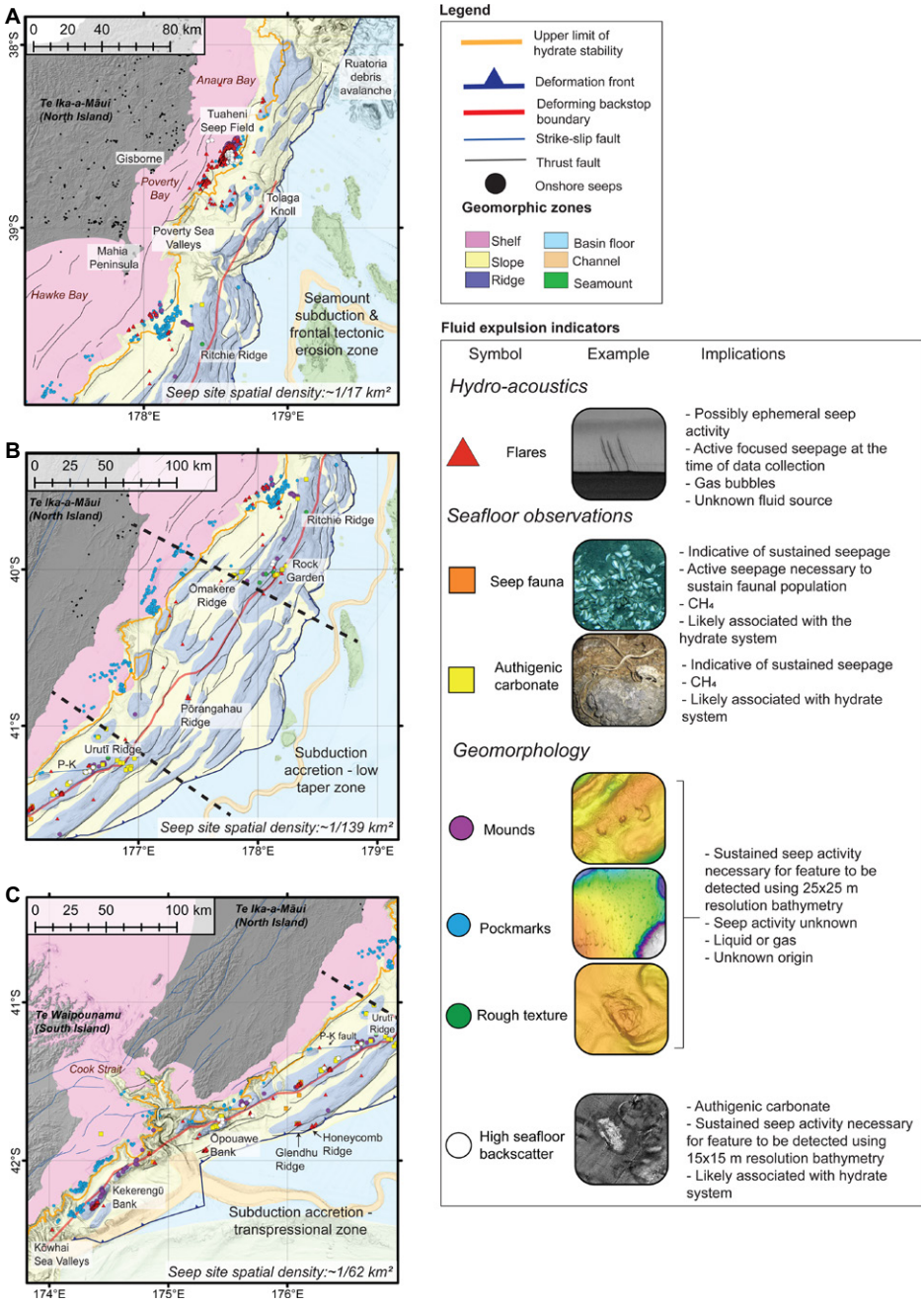

Figure 2. Maps showing distribution of fluid-expulsion indicators along the Hikurangi margin, offshore the North Island of New Zealand, according to broad-scale margin geomorphology. (A) Frontal tectonic erosion and seamount subduction zone. (B) Subduction accretion–low-taper zone. P-K—Palliser-Kaiwhata fault. (C) Subduction accretion–transpressional zone. Black dashed lines represent boundaries between the different tectonic domains on the Hikurangi margin. Please refer to Figure 1 and/or the Data Repository (see footnote 1) for mapped coverage of the multibeam bathymetry and water-column data on the margin. Features described in the text are labeled. Examples and implications of each fluid expulsion indicator presented in this study are provided in the legend. Seep site spatial density was calculated by dividing the total mapped area within the zone (km²) by the corresponding number of seepage indicators for that zone, presented as one seep indicator per unit area.

that intersect with the weakly coupled plate interface inland of the coast (Barnes et al., 2002; Mountjoy and Barnes, 2011). Active focused seepage between Rock Garden and Tolaga Knoll (Figs. 2A and 2B) lies landward of the frontal accretionary wedge and coincides with active thrust faulting and upper-plate fracture networks above and landward of subducting seamounts (Barnes et al., 2010; Pedley et al., 2010; Bell et al., 2010, 2014; Plaza-Faverola et al., 2014; Barker et al., 2018).

Zones of active focused seepage at North Hikurangi overlie regions characterized by microseismicity and tectonic tremor (Todd and Schwartz, 2016; Todd et al., 2018), shallow slow slip events (Wallace and Beavan, 2010; Wallace et al., 2016), and a highly reflective subducting unit that has been inferred to be fluid rich (Barker et al., 2009; Bell et al., 2010), moderately overpressured, and associated with seamount subduction (Fig. 1; Bassett et al., 2014; Ellis et al., 2015). Hydrofracturing at the inner-plate interface facilitates fluid drainage from the subducting sequence by providing secondary permeability in the overriding plate (Ellis et al., 2015), as supported by mantle/slab He isotope signatures in onshore fluid seeps (Reyes et al., 2010). Similarly, active seepage off the coast of Costa Rica is closely associated with subducted seamounts on the Cocos plate (Ranero et al.,

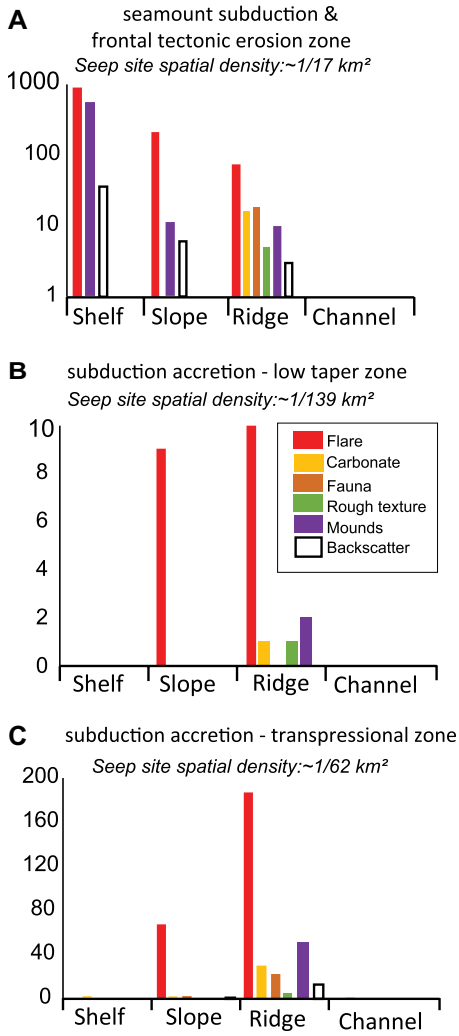

Figure 3. Bar graphs showing distribution of each fluid expulsion indicator as a function of geomorphic zones for (A) frontal tectonic erosion and seamount subduction zone, (B) subduction accretion–low-taper zone, and (C) subduction accretion–transpressional zone at the Hikurangi margin, offshore the North Island of New Zealand. Note the different *y*-axis scales in A–C. Refer to Figure 2 for the broad-scale margin morphology associated with these graphs. Seep site spatial density for each zone is annotated.

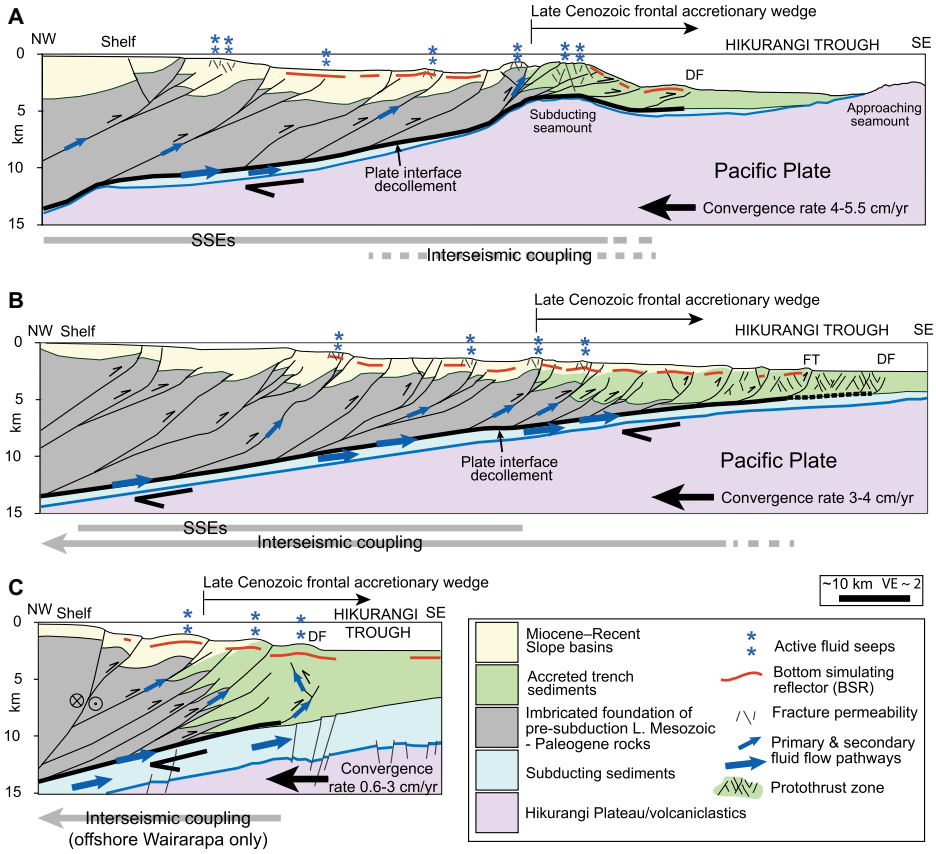

Figure 4. Conceptualized cross sections of the Hikurangi margin (offshore the North Island of New Zealand) illustrating along-strike variability in tectonic setting and stratigraphic architecture, representative active fluid seepage locations, and inferred major fluid-flow pathways. (A) Northern margin characterized by seamount subduction (adapted from sections in Barnes et al., 2002, 2010; Nicol et al., 2007). (B) Wide, accretionary central margin (adapted from sections in Barnes et al., 2002, 2010; Ghisetti et al., 2016; Plaza-Faverola et al., 2016). (C) Narrow, transpressive southern margin (adapted from sections in Plaza-Faverola et al., 2012; Bland et al., 2015; Kroeger et al., 2015). Convergence rates, slow slip events (SSEs), and interseismic coupling are from Wallace et al. (2004, 2012, 2016) and Wallace and Beavan (2010). Seep locations within each respective sector are projected along strike onto each section. Locations of the Deformation Front (DF) and Frontal Thrust (FT) are labeled.

2008; Sahling et al., 2008). Intriguingly, we observed no evidence for active focused seepage in the Poverty re-entrant, across the ~7000 km^2 Ruatoria re-entrant and associated debris-avalanche deposits, and in the Poverty Sea Valleys and canyons. These features are considered to have evolved from major impact scars (wake avalanches) associated with subducted seamounts (Fig. 2A; Lewis et al., 1998; Collot et al., 2001; Pedley et al., 2010). The chaotic nature of the debris-avalanche deposits may not favor localized fluid expulsion. We also observed a distinct lack of focused seepage on the relatively narrow (15–25 km), highly tapered (10°–15°) frontal accretionary wedge in the northern margin.

The wide (150 km), low-taper (4°) central margin wedge, characterized by a decreased orthogonal convergence rate (3–4 cm/yr) and increased sedimentary thickness on the subducting plate (3–4 km), has the lowest density of seepage observed on the margin (Figs. 2B and 3B). The absence of active focused seepage in this region, compared to the northern and southern areas, could be related to more distributed, diffuse and/or smaller-scale fluid expulsion, which may not be detectable in acoustic water-column backscatter data or at the scale measured in this study. Diffuse fluid expulsion has been documented to represent the majority of fluids expelled at some accretionary margins (e.g., Nankai and Barbados; Saffer and Bekins, 1998, 1999), and thus may also play a significant role in wedge dewatering of the central Hikurangi margin wedge. Hydroacoustic flares occur predominantly on thrust ridges deforming the presubduction foundation of the inner margin (Barnes et al., 2010; Pecher et al., 2010). These fluids may reflect microbial methanogenesis coupled with shallow permeable pathways and/or fluids released from compaction of subducting sediments, and clay dehydration reactions (e.g., Bekins et al., 1994; Hyndman et al., 1997; Reyes et al., 2010; Plaza-Faverola et al., 2016), with upward flow along structure-induced permeability (Fig. 4B; Barnes et al., 2010).

To the south, the margin-normal convergence rate decreases nearly fourfold, from ~3 to 0.6 cm/yr, and the wedge narrows from ~100 km to ~40 km wide (Fig. 1). Focused seepage extends to the deformation front at Honeycomb Ridge, and up to 130 km farther south than previously recognized along the midslope Kekerengū Bank thrust ridge (Fig. 2C). While seep sites at Urutī Ridge are proximal to the northern strike-slip section of the Palliser-Kaiwhata fault, no seepage was observed directly along the other major strike-slip faults of the southern margin (Fig. 2C). A correlation was found, however, between the distribution of fluid seepage on thrust ridges and the spatial distribution of concentrated gas hydrate indicators in regional seismic data (cf. Crutchley et al., 2019). We surmise that deforming thrust ridges in this context are more efficient wedge dewatering structures than strike-slip faults or are more effective structural traps for migrating fluids, enabling the development of productive seep environments. Although strike-slip faults have been previously considered to be effective dewatering conduits in other accretionary settings (e.g., Wecoma fault, Oregon; Tobin et al., 1993), the lack of observed focused seepage along such faults on the southern margin supports the notion that fluid expulsion along strike-slip margins is relatively sparse compared to subduction settings (Fig. 4C; Maloney et al., 2015).

We observed an overall lack of evidence for focused fluid seepage across the Hikurangi margin frontal wedge, despite rapid accretion of thick trench sediments (Fig. 2B; Ghisetti et al., 2016), and the expectation of compaction-driven dewatering dominating fluid sources (Saffer and Bekins, 2006; Ellis et al., 2015). At least 90% of observed seepage occurs above the deforming Late Cretaceous–Paleogene foundation, and it is most prevalent ~20–70 km landward of the deformation front (Figs. 2A–2C). The absence of focused seepage across the central margin frontal wedge may reflect poor drainage, resulting in elevated fluid pressures, a relatively weak plate interface, and low-taper (2°–4°) morphology (Fig. 4B). Alternatively, dewatering of the central Hikurangi margin and frontal wedge manifests predominantly as diffuse seepage, below our detection threshold (cf. Nankai accretionary margin; Saffer and Bekins, 1998). Low-taper, stable accretionary wedges typical of the central Hikurangi margin are thought to reflect poorly drained systems with a basal fault zone that is either fluid overpressured or frictionally weak, relative to the wedge (Dahlen, 1990; Sibson and Rowland, 2003; Ellis et al., 2019). We note that the wide low-taper Washington sector of the Cascadia margin has a similar distribution of seepage (Riedel et al., 2018) and strong interseismic coupling (Schmalzle et al., 2014). Active focused seepage on the Hikurangi margin does not show any obvious spatial relationship

with the slow slip events and/or interseismic coupling (Figs. 1 and 2A–2C).

CONCLUSIONS

Active focused seepage along the Hikurangi margin manifests mostly above the deforming backstop, likely exploits tectonically generated conduits that disrupt regional gas hydrate stability, and is largely absent from the frontal wedge. Patterns of seepage vary in accordance with changes in subduction setting (from the subduction accretion–transpressional zone, to subduction accretion–low-taper zone, and finally to seamount subduction and frontal tectonic erosion zone), convergence rate, and subducting plate roughness and sediment thickness. North-to-south variations in focused seepage observed in the current data set support previous suggestions that changes in subduction processes influence structural permeability and drainage pathways. We expect that large-scale seafloor seepage patterns may provide important insights into the deeper mechanics of accretionary and nonaccretionary systems.

ACKNOWLEDGMENTS

Data used for this study came from a large number of marine surveys using several different vessels, but primarily RV *Tangaroa*. We are grateful to the science officers and ship officers and crew staffing those surveys for the provision of the accumulated survey data that underpin this study. Some of the data collection and analysis was funded by New Zealand Petroleum and Minerals (NZP&M) for two petroleum basin screening reports (Bland et al., 2014; Crutchley et al., 2016). We are grateful to OMV New Zealand (Wellington) for providing access to multibeam data from the inner central margin. Funding for National Institute of Water and Atmospheric Research (NIWA) staff came from the Ministry of Business, Innovation, and Employment (MBIE) Strategic Science Investment Fund (SSIF) Marine Geological Processes Programme of the NIWA Coasts and Oceans Centre. Funding for Crutchley and Hillman, and partially for Watson and Mountjoy, was provided by the New Zealand MBIE Endeavor Fund Programme Gas Hydrates: Economic Opportunities and Environmental Impact (HYDEE; contract CO5X1708). We thank D. Saffer and two anonymous reviewers for their constructive feedback that greatly improved this manuscript.

REFERENCES CITED

Bangs, N.L., McIntosh, K.D., Silver, E.A., Kluesner, J.W., and Ranero, C.R., 2015, Fluid accumulation along the Costa Rica subduction thrust and development of the seismogenic zone: Journal of Geophysical Research–Solid Earth, v. 120, p. 67–86, https://doi.org/10.1002/2014JB011265.

Barker, D.H., Sutherland, R., Henrys, S., and Bannister, S., 2009, Geometry of the Hikurangi subduction thrust and upper plate, North Island, New Zealand: Geochemistry Geophysics Geosystems, v. 10, Q02007, https://doi.org/10.1029/2008GC002153 .

Barker, D.H., Henrys, S., Caratori Tontini, F., Barnes, P.M., Bassett, D., Todd, E., and Wallace, L., 2018, Geophysical constraints on the relationship between seamount subduction, slow slip, and tremor at the North Hikurangi subduction zone, New Zealand: Geophysical Research Letters, v. 45, p. 12–804, https://doi.org/10.1029/2018GL080259.

Barnes, P.M., Nicol, A., and Harrison, T., 2002, Late Cenozoic evolution and earthquake potential of an active listric thrust complex above the Hikurangi subduction zone, New Zealand: Geological Society of America Bulletin, v. 114, p. 1379–1405, https://doi.org/10.1130/0016-7606(2002)114<1379:LCEAEP>2.0.CO;2.

Barnes, P.M., Lamarche, G., Bialas, J., Henrys, S., Pecher, I., Netzeband, G.L., Greinert, J., Mountjoy, J.J., Pedley, K., and Crutchley, G., 2010, Tectonic and geological framework for gas hydrates and cold seeps on the Hikurangi subduction margin, New Zealand: Marine Geology, v. 272, p. 26–48, https://doi.org/10.1016/j.margeo.2009.03.012.

Barnes, P.M., Ghisetti, F.C., Ellis, S., and Morgan, J.K., 2018, The role of protothrusts in frontal accretion and accommodation of plate convergence, Hikurangi subduction margin, New Zealand: Geosphere, v. 14, p. 440–468, https://doi.org/10.1130/GES01552.1.

Bassett, D., Sutherland, R., and Henrys, S., 2014, Slow wavespeeds and fluid overpressure in a region of shallow geodetic locking and slow slip, Hikurangi subduction margin, New Zealand: Earth and Planetary Science Letters, v. 389, p. 1–13, https://doi.org/10.1016/j.epsl.2013.12.021.

Beavan, J., Tregoning, P., Bevis, M., Kato, T., and Meertens, C., 2002, Motion and rigidity of the Pacific plate and implications for plate boundary deformation: Journal of Geophysical Research–Solid Earth, v. 107, p. ETG 9-1, https://doi.org/10.1029/2001JB000282.

Bekins, B., McCaffrey, A.M., and Dreiss, S.J., 1994, Influence of kinetics on the smectite to illite transition in the Barbados accretionary prism: Journal of Geophysical Research–Solid Earth, v. 99, p. 18147–18158, https://doi.org/10.1029/94JB01187.

Bell, R., Sutherland, R., Barker, D.H., Henrys, S., Bannister, S., Wallace, L., and Beavan, J., 2010, Seismic reflection character of the Hikurangi subduction interface, New Zealand, in the region of repeated Gisborne slow slip events: Geophysical Journal International, v. 180, p. 34–48, https://doi.org/10.1111/j.1365-246X.2009.04401.x.

Bell, R., Holden, C., Power, W., Wang, X., and Downes, G., 2014, Hikurangi margin tsunami earthquake generated by slow seismic rupture over a subducted seamount: Earth and Planetary Science Letters, v. 397, p. 1–9, https://doi.org/10.1016/j.epsl.2014.04.005.

Bland, K.J., et al., 2014, Pegasus Basin Petroleum Prospectivity Screening Report: GNS Science Consultancy Report 2014/103, 139 p.

Bland, K.J., Uruski, C.I., and Isaac, M.J., 2015, Pegasus Basin, eastern New Zealand: A stratigraphic record of subsidence and subduction, ancient and modern: New Zealand Journal of Geology and Geophysics, v. 58, p. 319–343, https://doi.org/10.1080/00288306.2015.1076862.

Böttner, C., Gross, F., Geersen, J., Crutchley, G.J., Mountjoy, J.J., and Krastel, S., 2018, Marine forearc extension in the Hikurangi margin: New insights from high-resolution 3-D seismic data: Tectonics, v. 37, p. 1472–1491, https://doi.org/10.1029/2017TC004906.

Campbell, K.A., 2006, Hydrocarbon seep and hydrothermal vent paleoenvironments and paleontology: Past developments and future research directions: Palaeogeography, Palaeoclimatology, Palaeoecology, v. 232, p. 362–407, https://doi.org/10.1016/j.palaeo.2005.06.018.

Campbell, K.A., Francis, D.A., Collins, M., Gregory, M.R., Nelson, C.S., Greinert, J., and Aharon, P., 2008, Hydrocarbon seep-carbonates of a Miocene forearc (East Coast Basin), North Island, New Zealand: Sedimentary Geology, v. 204, p. 83–105, https://doi.org/10.1016/j.sedgeo.2008.01.002.

Collot, J.-Y., Delteil, J., Lewis, K.B., Davy, B., Lamarche, G., Audru, J.-C., Barnes, P., Chanier, F., Chaumillon, E., and Lallemand, S., 1996, From oblique subduction to intra-continental transpression: Structures of the southern Kermadec-Hikurangi margin from multibeam bathymetry, side-scan sonar and seismic reflection: Marine Geophysical Researches, v. 18, p. 357–381, https://doi.org/10.1007/BF00286085.

Collot, J.-Y., Lewis, K., Lamarche, G., and Lallemand, S., 2001, The giant Ruatoria debris avalanche on the northern Hikurangi margin, New Zealand: Result of oblique seamount subduction: Journal of Geophysical Research: Solid Earth, v. 106, p. 19271–19297, https://doi.org/10.1029/2001JB900004.

Crutchley, G.J., et al., 2016, Petroleum Prospectivity Screening Report of the offshore Northern East Coast Basin: GNS Science Consultancy Report 2015/225.

Crutchley, G.J., Kroeger, K.F., Pecher, I.A., and Gorman, A.R., 2019, How tectonic folding influences gas hydrate formation: New Zealand's Hikurangi subduction margin: Geology, v. 47, p. 39–42, https://doi.org/10.1130/G45151.1.

Dahlen, F.A., 1990, Critical taper model of fold-and-thrust belts and accretionary wedges: Annual Review of Earth and Planetary Sciences, v. 18, p. 55–99, https://doi.org/10.1146/annurev.ea.18.050190.000415.

Ellis, S., Fagereng, A., Barker, D., Henrys, S., Saffer, D., Wallace, L., Williams, C., and Harris, R., 2015, Fluid budgets along the northern Hikurangi subduction margin, New Zealand: The effect of a subducting seamount on fluid pressure: Geophysical Journal International, v. 202, p. 277–297, https://doi.org/10.1093/gji/ggv127.

Ellis, S., Ghisetti, F., Barnes, P.M., Boulton, C., Fagereng, A., and Buiter, S., 2019, The contemporary force balance in a wide accretionary wedge: numerical models of the southcentral Hikurangi margin of New Zealand: Geophysical Journal International, v. 219, p. 776–795, https://doi.org/10.1093/gji/ggz317.

Fagereng, Å., 2011, Wedge geometry, mechanical strength, and interseismic coupling of the Hikurangi subduction thrust, New Zealand: Tectonophysics, v. 507, p. 26–30, https://doi.org/10.1016/j.tecto.2011.05.004.

Geersen, J., Ranero, C.R., Klaucke, I., Behrmann, J.H., Kopp, H., Tréhu, A.M., Contreras-Reyes, E., Barckhausen, U., and Reichert, C., 2018, Active tectonics of the North Chilean marine forearc and adjacent oceanic Nazca Plate: Tectonics, v. 37, p. 4194–4211, https://doi.org/10.1029/2018TC005087.

Ghisetti, F.C., Barnes, P.M., Ellis, S., Plaza-Faverola, A.A., and Barker, D.H., 2016, The last 2 Myr of accretionary wedge construction in the central Hikurangi margin (North Island, New Zealand): Insights from structural modeling: Geochemistry Geophysics Geosystems, v. 17, p. 2661–2686, https://doi.org/10.1002/2016GC006341.

Greinert, J., Lewis, K.B., Bialas, J., Pecher, I.A., Rowden, A., Bowden, D.A., De Batist, M., and Linke, P., 2010, Methane seepage along the Hikurangi Margin, New Zealand: Overview of studies in 2006 and 2007 and new evidence from visual, bathymetric and hydroacoustic investigations: Marine Geology, v. 272, p. 6–25, https://doi.org/10.1016/j.margeo.2010.01.017.

Higgs, B., Mountjoy, J.J., Crutchley, G.J., Townend, J., Ladroit, Y., Greinert, J., and McGovern, C., 2019, Seep-bubble characteristics and gas flow rates

from a shallow-water, high-density seep field on the shelf-to-slope transition of the Hikurangi subduction margin: Marine Geology, v. 417, https://doi.org/10.1016/j.margeo.2019.105985.

Hyndman, R.D., Yamano, M., and Oleskevich, D.A., 1997, The seismogenic zone of subduction thrust faults: The Island Arc, v. 6, p. 244–260, https://doi.org/10.1111/j.1440-1738.1997.tb00175.x.

Judd, A., and Hovland, M., (2009). Seabed Fluid Flow: The Impact on Geology, Biology and the Marine Environment: Cambridge, UK, Cambridge University Press.

Kodaira, S., Iidaka, T., Kato, A., Park, J.-O., Iwasaki, T., and Kaneda, Y., 2004, High pore fluid pressure may cause silent slip in the Nankai Trough: Science, v. 304, p. 1295–1298, https://doi.org/10.1126/science.1096535.

Kroeger, K.F., Plaza-Faverola, A., Barnes, P.M., and Pecher, I.A., 2015, Thermal evolution of the New Zealand Hikurangi subduction margin: Impact on natural gas generation and methane hydrate formation–a model study: Marine and Petroleum Geology, v. 63, p. 97–114, https://doi.org/10.1016/j.marpetgeo.2015.01.020.

Lewis, K.B., and Marshall, B.A., 1996, Seep faunas and other indicators of methane-rich dewatering on New Zealand convergent margins: New Zealand Journal of Geology and Geophysics, v. 39, p. 181–200, https://doi.org/10.1080/00288306.1996.9514704.

Lewis, K.B., and Pettinga, J.R., 1993, The emerging, imbricate frontal wedge of the Hikurangi margin: Sedimentary Basins of the World, v. 2, p. 225–250.

Lewis, K.B., Collot, J.-Y., and Lallemand, S.E., 1998, The dammed Hikurangi Trough: A channel-fed trench blocked by subducting seamounts and their wake avalanches (New Zealand–France GeodyNZ Project): Basin Research, v. 10, p. 441–468, https://doi.org/10.1046/j.1365-2117.1998.00080.x.

Liu, Y., and Rice, J.R., 2007, Spontaneous and triggered aseismic deformation transients in a subduction fault model: Journal of Geophysical Research: Solid Earth, v. 112, B09404, https://doi.org/10.1029/2007JB004930.

Maloney, J.M., Grupe, B.M., Pasulka, A.L., Dawson, K.S., Case, D.H., Frieder, C.A., Levin, L.A., and Driscoll, N.W., 2015, Transpressional segment boundaries in strike-slip fault systems offshore southern California: Implications for fluid expulsion and cold seep habitats: Geophysical Research Letters, v. 42, p. 4080–4088, https://doi.org/10.1002/2015GL063778.

Mountjoy, J.J., and Barnes, P.M., 2011, Active upper plate thrust faulting in regions of low plate interface coupling, repeated slow slip events, and coastal uplift: Example from the Hikurangi Margin, New Zealand: Geochemistry Geophysics Geosystems, v. 12, https://doi.org/10.1029/2010GC003326.

Nicol, A., Mazengarb, C., Chanier, F., Rait, G., Uruski, C., and Wallace, L., 2007, Tectonic evolution of the active Hikurangi subduction margin, New Zealand, since the Oligocene: Tectonics, v. 26, https://doi.org/10.1029/2006TC002090.

Pecher, I.A., Henrys, S.A., Wood, W.T., Kukowski, N., Crutchley, G.J., Fohrmann, M., Kilner, J., Senger, K., Gorman, A.R., and Coffin, R.B., 2010, Focused fluid flow on the Hikurangi Margin, New Zealand—Evidence from possible local upwarping of the base of gas hydrate stability: Marine Geology, v. 272, p. 99–113, https://doi.org/10.1016/j.margeo.2009.10.006.

Pedley, K.L., Barnes, P.M., Pettinga, J.R., and Lewis, K.B., 2010, Seafloor structural geomorphic evolution of the accretionary frontal wedge in response to seamount subduction, Poverty Indentation, New Zealand: Marine Geology, v. 270, p. 119–138, https://doi.org/10.1016/j.margeo.2009.11.006.

Plaza-Faverola, A., Klaeschen, D., Barnes, P., Pecher, I., Henrys, S., and Mountjoy, J., 2012, Evolution of fluid expulsion and concentrated hydrate zones across the southern Hikurangi subduction margin, New Zealand: An analysis from depth migrated seismic data: Geochemistry Geophysics Geosystems, v. 13, https://doi.org/10.1029/2012GC004228.

Plaza-Faverola, A., Pecher, I., Crutchley, G., Barnes, P.M., Bünz, S., Golding, T., Klaeschen, D., Papenberg, C., and Bialas, J., 2014, Submarine gas seepage in a mixed contractional and shear deformation regime: Cases from the Hikurangi oblique-subduction margin: Geochemistry Geophysics Geosystems, v. 15, p. 416–433, https://doi.org/10.1002/2013GC005082.

Plaza-Faverola, A., Henrys, S., Pecher, I., Wallace, L., and Klaeschen, D., 2016, Splay fault branching from the Hikurangi subduction shear zone: Implications for slow slip and fluid flow: Geochemistry Geophysics Geosystems, v. 17, p. 5009–5023, https://doi.org/10.1002/2016GC006563.

Ranero, C.R., Grevemeyer, I., Sahling, H., Barckhausen, U., Hensen, C., Wallmann, K., Weinrebe, W., Vannucchi, P., Von Huene, R., and McIntosh, K., 2008, Hydrogeological system of erosional convergent margins and its influence on tectonics and interplate seismogenesis: Geochemistry Geophysics Geosystems, v. 9, https://doi.org/10.1029/2007GC001679.

Reyes, A.G., Christenson, B.W., and Faure, K., 2010, Sources of solutes and heat in low-enthalpy mineral waters and their relation to tectonic setting, New Zealand: Journal of Volcanology and Geothermal Research, v. 192, p. 117–141, https://doi.org/10.1016/j.jvolgeores.2010.02.015.

Riedel, M., Scherwath, M., Römer, M., Veloso, M., Heesemann, M., and Spence, G.D., 2018, Distributed natural gas venting offshore along the Cascadia margin: Nature Communications, v. 9, p. 3264, https://doi.org/10.1038/s41467-018-05736-x.

Saffer, D.M., and Bekins, B.A., 1998, Episodic fluid flow in the Nankai accretionary complex: Timescale, geochemistry, flow rates, and fluid budget: Journal of Geophysical Research: Solid Earth, v. 103, p. 30351–30370, https://doi.org/10.1029/98JB01983.

Saffer, D.M., and Bekins, B.A., 1999, Fluid budgets at convergent plate margins: Implications for the extent and duration of fault-zone dilation: Geology, v. 27, p. 1095–1098, https://doi.org/10.1130/0091-7613(1999)027<1095:FBACPM>2.3.CO;2.

Saffer, D.M., and Bekins, B.A., 2006, An evaluation of factors influencing pore pressure in accretionary complexes: Implications for taper angle and wedge mechanics: Journal of Geophysical Research: Solid Earth, v. 111, B04101, https://doi.org/10.1029/2005JB003990.

Saffer, D.M., and Tobin, H.J., 2011, Hydrogeology and mechanics of subduction zone forearcs: Fluid flow and pore pressure: Annual Review of Earth and Planetary Sciences, v. 39, p. 157–186, https://doi.org/10.1146/annurev-earth-040610-133408.

Sahling, H., Masson, D.G., Ranero, C.R., Hühnerbach, V., Weinrebe, W., Klaucke, I., Bürk, D., Brückmann, W., and Suess, E., 2008, Fluid seepage at the continental margin offshore Costa Rica and southern Nicaragua: Geochemistry Geophysics Geosystems, v. 9, https://doi.org/10.1029/2008GC001978.

Schmalzle, G.M., McCaffrey, R., and Creager, K.C., 2014, Central Cascadia subduction zone creep: Geochemistry Geophysics Geosystems, v. 15, p. 1515–1532, https://doi.org/10.1002/2013GC005172.

Sibson, R.H., 1992, Fault-valve behavior and the hydrostatic-lithostatic fluid pressure interface: Earth-Science Reviews, v. 32, p. 141–144, https://doi.org/10.1016/0012-8252(92)90019-P.

Sibson, R.H., and Rowland, J.V., 2003, Stress, fluid pressure and structural permeability in seismogenic crust, North Island, New Zealand: Geophysical Journal International, v. 154, p. 584–594, https://doi.org/10.1046/j.1365-246X.2003.01965.x.

Tobin, H.J., Moore, J.C., Mackay, M.E., Orange, D.L., and Kulm, L.D., 1993, Fluid flow along a strike-slip fault at the toe of the Oregon accretionary prism: Implications for the geometry of frontal accretion: Geological Society of America Bulletin, v. 105, p. 569–582, https://doi.org/10.1130/0016-7606(1993)105<0569:FFAASS>2.3.CO;2.

Todd, E.K., and Schwartz, S.Y., 2016, Tectonic tremor along the northern Hikurangi Margin, New Zealand, between 2010 and 2015: Journal of Geophysical Research: Solid Earth, v. 121, p. 8706–8719, https://doi.org/10.1002/2016JB013480.

Todd, E.K., Schwartz, S.Y., Mochizuki, K., Wallace, L.M., Sheehan, A.F., Webb, S.C., Williams, C.A., Nakai, J., Yarce, J., and Fry, B., 2018, Earthquakes and tremor linked to seamount subduction during shallow slow slip at the Hikurangi margin, New Zealand: Journal of Geophysical Research: Solid Earth, v. 123, p. 6769–6783, https://doi.org/10.1029/2018JB016136.

Wallace, L.M., and Beavan, J., 2010, Diverse slow slip behavior at the Hikurangi subduction margin, New Zealand: Journal of Geophysical Research: Solid Earth, v. 115, B12402, https://doi.org/10.1029/2010JB007717.

Wallace, L.M., Beavan, J., McCaffrey, R., and Darby, D., 2004, Subduction zone coupling and tectonic block rotations in the North Island, New Zealand: Journal of Geophysical Research: Solid Earth, v. 109, B12406, https://doi.org/10.1029/2004JB003241.

Wallace, L.M., Barnes, P., Beavan, J., Van Dissen, R., Litchfield, N., Mountjoy, J., Langridge, R., Lamarche, G., and Pondard, N., 2012, The kinematics of a transition from subduction to strike-slip: An example from the central New Zealand plate boundary: Journal of Geophysical Research: Solid Earth, v. 117, https://doi.org/10.1029/2011JB008640.

Wallace, L.M., Webb, S.C., Ito, Y., Mochizuki, K., Hino, R., Henrys, S., Schwartz, S.Y., and Sheehan, A.F., 2016, Slow slip near the trench at the Hikurangi subduction zone, New Zealand: Science, v. 352, p. 701–704, https://doi.org/10.1126/science.aaf2349.

Wallace, L.M., Hreinsdóttir, S., Ellis, S., Hamling, I., D'Anastasio, E., and Denys, P., 2018, Triggered slow slip and afterslip on the southern Hikurangi subduction zone following the Kaikōura earthquake: Geophysical Research Letters, v. 45, p. 4710–4718, https://doi.org/10.1002/2018GL077385.

Printed in USA